Journal of the Serbian Chemical Society
JSCS-info@shd.org.rs • www.shd.org.rs/JSCS
J. Serb. Chem. Soc. *86* (6) 561–570 (2021)
JSCS–5443
Original scientific paper

3D-QSAR study of adenosine 5'-phosphosulfate (APS) analouges as ligands for APS reductase

SLAVICA ERIĆ[1]*, ILIJA CVIJETIĆ[2] and MIRE ZLOH[3,4]

[1]*University of Belgrade – Faculty of Pharmacy, Vojvode Stepe 450, 11221 Belgrade, Serbia,* [2]*University of Belgrade – Innovation Center of the Faculty of Chemistry, Studentski trg 12–16, 11000 Belgrade, Serbia,* [3]*Nanopuzzle Medicines Design, Stevenage, United Kingdom and* [4]*Faculty of Pharmacy, University Business Academy, Novi Sad, Serbia*

(Received 28 November 2020, revised 21 January, accepted 26 February 2021)

Abstract: Metabolism of sulfur (sulfur assimilation pathway, SAP) is one of the key pathways for the pathogenesis and survival of persistant bacteria, such as *Mycobacterium tuberculosis* (Mtb), in the latent period. Adenosine 5'-phosphosulfate reductase (APSR) is an important enzyme involved in the SAP, absent from the human body, so it might represent a valid target for development of new antituberculosis drugs. This work aimed to develop 3D-QSAR model based on the crystal structure of APSR from *Pseudomonas aeruginosa*, which shows high degree of homology with APSR from Mtb, in complex with its substrate, adenosine 5'-phosphosulfate (APS). 3D-QSAR model was built from a set of 16 nucleotide analogues of APS using alignment-independent descriptors derived from molecular interaction fields (MIF). The model improves the understanding of the key characteristics of molecules necessary for the interaction with target, and enables the rational design of novel small molecule inhibitors of Mtb APSR.

Keywords: sulfur assimilation pathway; interactions; MIF; pentacle; PLS.

INTRODUCTION

Various studies showed that the metabolic pathway of sulfur (sulfur assimilation pathway, SAP) is crucial for the survival of persistant bacteria, such as *Mycobacterium tuberculosis* (Mtb) in the latent period, after adaptation on primary cell response from the host.[1–3] This pathway provides reduced form of sulfur which serves for biosynthesis of a number of metabolites, including cysteine, methionine, various coenzymes, as well as mycothiol.[4] The metabolic pathway of sulfur starts with the active transport of sulfates catalyzed by sulfate-permease. Adenylation catalyzed by ATP sulfurylase (CysD) yields adenosine-5‘-phosphosulfate (APS). This product is then converted to sulfite and adenosine by APS-

* Corresponding author. E-mail: seric@pharmacy.bg.ac.rs
https://doi.org/10.2298/JSC201128015E

reductase (APSR), with cofactor thioredoxin.[5] APSR is not synthetized in human organism, therefore could be one of the selective targets for blocking sulfur metabolic pathway. Upregulation of CysH, that codes APSR, was observed during the resting state of bacteria, as well as during exposition to hydrogen peroxide and starving, which suggests that APSR is activated immediately after the initial infection and allows survival of bacteria.[6]

Recently, small-molecule inhibitors of APS reductase were discovered through virtual ligand screening.[7] However, it was stated that the development of more specific and potent inhibitors would be greatly aided through knowledge of the functional importance of interactions between the substrate and enzyme at the active site. For that purpose, several analogues of APS were synthetized and their affinities for APSR were experimentally determined. These studies define chemical groups that are essential for molecular recognition and reveal a network of electrostatic interactions, which play an important role in substrate discrimination. To gain further insight into substrate recognition of Mtb APS reductase, energetic contribution of individual portions of APS to the enzyme-binding interaction was analyzed.

For further contribution in design of APSR inhibitors, we used 16 synthetized analogues with determined K_d values for generation of pharmacophoric model based on interactions of ligands with the active site of homologous APSR. Since three-dimensional structure of Mtb APSR is not known, we used the structure of APS in complex with APSR of *Pseudomonas aeruginosa*, that shows high degree of homology (27.2 % identical sequences and 41.4 % similar). As expected for phylogenetically related proteins, the highest degree of similarity was observed for the APSR active site residues.[6] Using a known structure of natural substrate for APSR and its 16 structural analogues, alignment-independent 3D-QSAR model was developed from the MIF-based descriptors. The model was interpreted in order to elucidate interactions between APS analogues and APSR. The obtained pharmacophoric hot-spots could serve as the basis for rational design of novel APSR inhibitors.

EXPERIMENTAL

The structure of APS ligand was retrieved from the complex with APSR from *P. aeruginosa* (PDB code 2GOY). Since three-dimensional (3D) crystal structure of APSR of Mtb is not defined, structural data from the complex of APS with *P. aeruginosa*, showing high degree of homology,[8] were utilized for QSAR studies.

The set of 16 APS analogues, along with their K_d values are collected from literature[5] and in house laboratory data that are not published yet. The conformer ensemble for each molecule was generated by Omega – e,[9,10] and conformers most similar to the conformation of natural APS ligand were selected by vROCS.[11,12] These conformers were used for generation of 3D-QSAR models, computing GRIND descriptors from the encoded molecular interaction fields (MIF) in Pentacle program.[13] MIFs characterize the interaction features of a molecule with the environment which could be mapped using chemical probes. Four mole-

cular probes mapping different chemical/pharmacophoric features of ligands were applied in this study: DRY probe that simulates hydrophobic interactions of molecules with active center of the target; N1 probe (amide nitrogen) mapping hydrogen-bonding acceptors (HBA) of a ligand; O probe (carbonyl oxygen) mapping hydrogen-bonding donors (HBD), and TIP probe showing what shape of the molecules fits within the active center of the enzyme. The MIFs are computed by placing the molecule in a grid having certain, predefined resolution. The chemical probes are then positioned at each nodal point and the corresponding interaction energy is computed. Obtained interaction energies represent the molecular descriptors of hydrophobic, hydrogen bonding interactions, and shape complementarity with the protein target.

RESULTS AND DISCUSSION

Chartron *et al.* published 3D crystal structure of APSR of bacterium *P. aeruginosa* in complex with the substrate (APS).[14] APSR of *P. aeruginosa* and *M. tuberculosis* show high degree of homology (27.2 % of identical sequences and 41.4 % of similar), especially within the active site. This structure was the base for investigation of significant interactions between enzyme and substrate, which could give an idea for rational design of potential APSR inhibitors.

Hong *et al.*[5] performed structure–activity study of various substrates and product analogues in order to analyse molecular determinants important for binding and specificity on APSR. Study showed that binding of dianions is more favorable compared to monoanions. Analysis of adenosine, D-ribose and adenine fragments showed that they exhibit weak binding affinity comparing to the whole molecule. Detailed study of substrates and products showed: loss of sulphate reduces binding affinity, β-sulphate groups play a modest role in recognition of substrate, sulphur substitution is considered to be a good mimic of the phosphate moiety because it is isosteric, pseudoisoelectronic, and similar charge distribution and net charge at physiological pH. Contribution of α–β bridging oxygen was analysed in respect to geometry, charge density and distribution, as well as ionization state of the molecules. The substitution of α-nonbridging oxygen by sulphur, indicated possible disruption of contacts with residues, which could be important for stabilizing charge development in transition state. The similarity of Kd for different analogues, however, could possibly indicate the different modes of nucleotide binding, so further studies should be performed for detailed mechanisms of action.

This study provides additional insights into ligand binding to APSR. The hydrophobic, shape and hydrogen bonding properties of 16 nucleotide analogues of APS (Table S-I of the Supplementary material to this paper) are quantified by computing GRID molecular interaction fields (MIFs). This ligand-based approach utilized the bioactive conformation of APS in complex with P. aeruginosa APSR. The most similar conformation was extracted from the conformer ensemble of ligands and used for model generation. The interaction profiles are encoded into alignment-independent GRIND independent descriptors (GRid) descriptors and correlated with inhibitory activities to develop 3D-QSAR models.[5,7] GRIND

descriptors describe the most important network interactions as a function of distance instead of describing precise position of every point in the net.

Compounds from the data set were classified, on the basis of structural similarity, into three main groups: 1) adenosine 5'-monophosphate (AMP) and analogues: 3'-AMP, 5'-AMP, AMPS, AMPCF2P, AMPCP, AMPNP and AMPPN; 2) adenosine 5'-diphosphate (ADP) and analogues: 3',5'-ADP, ADPαS, ADPβS and ADPβF; 3) APS and analogues: APSαS and APSβM. Structural modifications in analogues are explained in the text.[5]

The large differences in APSR inhibitory activity were observed between three classes of compounds, indicating that slight differences in structure lead to significant changes in protein-ligand binding. For example, the K_d values for APS, ADP and AMP are 0.2, 4.3 and 5.4 μM, respectively. Following classification of compounds, the groups of ligands were further investigated. APS is a natural ligand of APS reductases with K_d value of 0.2 μM. Replacing sulfate group of APS with phosphate, as it is in the case of ADP, or by elimination of that group in AMP, the affinity for APS reductase decreases, which proves the importance of this group. Phosphate and sulfate groups are of similar size and shape, and they differ in the net charge. Sulfate group is mono-anion (charge –1) whilst phosphate group is di-anion (charge –2). Additional insights into the important structural and pharmacophoric features were obtained from the3D-QSAR model.

The preliminary SAR complemented by the analysis of GRIND descriptors

Fig. 1 shows all interactions that natural ligand APS might form with the active site of APSR, including possibility of hydrophobic interactions, H-bond donors, H-bond acceptors, as well as favorable shape of the molecule.

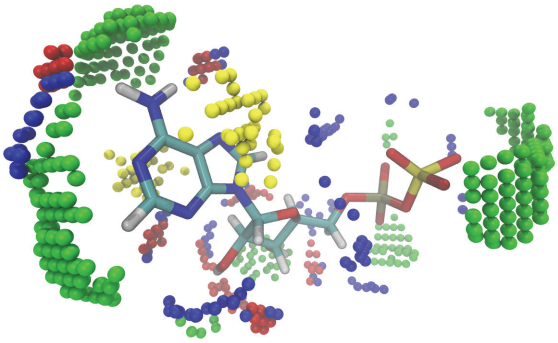

Fig. 1. Interactions of APS and active place of APSR: hydrophobic interactions (yellow), H-bond donors (blue), H-bond acceptors (red), MIFs describing the favorable shape of the molecule (green).

Concerning shape analysis, the significant differences were observed between APS, ADP and AMP. The most significant differences are observed between 6.8 and 10.4 Å, where APS shows significant shape complementarity

while ADP do not exert such interactions and do not completely fit within the active site.

The net charge for AMP and APS is the same, –2, which is a prerequisite for excellent binding to APSR.[5] Similar binding of two ligands is visible in TIP–TIP correlograms, where AMP shows favorable regions. The difference is that the charge of AMP is localized in *α*-position, and the implications of such charge arrangement on binding affinity will be further discussed.

The analysis of hydrophobic interactions indicated that purine part of the ligand is responsible for the hydrophobic interactions with the active site of enzyme. The heatmaps of DRY–DRY interactions show that APS forms the weakest hydrophobic interactions on short distance (between 3.8 and 5.6 Å), whilst interactions with ADP are the strongest. This could be the consequence of the particular conformation of ADP that enables intramolecular hydrogen bonding between the oxygen on *β*-phosphate and –NH at position 2 of purine ring. We suppose that additional intramolecular bonding decreases the overall binding affinity for APSR. As the position 2 of purine ring does not establish energetically favorable interactions within the APS reductase active site,[5] its modification to =CH– will probably lead to more potent analogues.

To study whether the decreased binding affinity of ADP is connected with additional charge of phosphate group in *β*-position, we further evaluated how the replacement of negatively charged oxygen (ADP) with sulfur (ADPβS) or fluorine (ADPβF) atoms influence the binding affinity. Two analogues show higher degree of binding for APS reductase, whilst significant improvement is observed for compound ADPβS. Higher affinity of ADPβS compared to ADPβF might be explained by larger size and polarizability of S atom. This substitution might enable the additional interactions that improve fitting of ligand in the active site. Additional hydrophobic interactions could be observed at the distances from 4.0 to 5.6 Å and 8.0–9.6 Å.

The replacement of negatively charged oxygen in *α*-position of ADP with sulfur also increases the binding affinity. Better shape complementarity of ADPαS with the active site is observed in the range between 7.2 and 12.0 Å.

The introduction of phosphate at 3'-OH of ribose yields 3'5'-ADP with significantly decreased binding energy. The changes in the skeleton of the molecule imposed by the introduction of additional ribose moiety reflect in the restricted conformational freedom and possibly lower fit with the APS reductase. Weaker DRY–DRY interactions of 3'5'-ADP compared to ADP and ADPβS are observed at the distance range from 4.4 to 9.6, suggesting that certain portion of important hydrophobic interactions are missing.

Concerning APS analogues, modification of APS in *α* and *β*-positions decreases the binding energy. In general, APSαS can be a substrate for APSR, but in the case of saturation of enzyme with the substrate there is no evidence that inter-

medier, *S*-sulfocysteine, could be formed.[5] It is not clear why APSR does effectively reduce APSαS. By analogy with *α*-S substitution in ADP, one of the explanations would be that the added S is an obstacle for contact with amino acid residues of active center of enzyme, while at the same time allowing the formation of some unfavorable hydrophobic interactions at the distance range from 3.6 to 5.6 and 7.6–9.2 Å.

In APSβM, oxygen bridge was replaced with methylene with an idea to explain the importance of this bridge during binding with enzyme. The binding energy decreased significantly, and the reason could be that methylene bridge increases the length of S–X–P bond and decreases the angle of rotation. It is also reflected as an increase in hydrophobic interactions with APSR between 4.4 and 5.6 Å and 7.6 and 8.4 Å. In further text, the importance of oxygen bridge will be explained through the analysis of AMP and its analogues.

The AMP is an important part of APS and plays role in enzyme recognition. However, the binding affinity of AMP for APSR is smaller comparing to ADP and ASP. It indicates that P*α*–O–S*β* bridge is essential for the activity. To determine the importance of oxygen in the bridge we compared the following AMP analogues: AMPCP, AMPCF2P and AMPNP. Each derivative has smaller binding affinity comparing to ADP and ASP. Among those analogues, the highest affinity is observed for AMPCF2P and lowest for AMPNP. However, concerning the size of AMPNP, it fits better within active site of enzyme than AMPCF2P, as observed on heatmaps of TIP–TIP interactions at the distance between 4.4 and 8.6 Å. It could be the consequence of voluminous $–CF_2–$ bridge that hinders fitting of compound into active site.

The neutralization of negatively charged oxygen in *β*-position decreases the activity. Consequently, the activity of AMPPN is significantly lower than the activity of AMPNP. On DRY–DRY correlograms, it can be seen that AMPPN forms weak hydrophobic interactions at the distance between 4.0 and 5.6 Å, and 8.4 and 9.6 Å, opposite to AMPNP. This trend might be explained by the protonation of *β*-NH_2 group at physiological pH and subsequent formation of intramolecular electrostatic interactions that prevent ligand binding to enzyme.[5]

The influence of *α*-substituents was further investigated by comparing the biological activities of AMP and *α*-substituted derivatives with sulfur (5'-AMPS) or amino group (5'-AMPN). Better shape complementarity of 5'-AMPS compared to AMP is indicated though stronger TIP–TIP interactions between 12.0 and 14.4 Å, allowing better fit into the APS reductase active site and lower K_d values (3.3 *vs*. 5.4 μM).

A significant decrease in binding affinity of 5'-AMPN analogue might also be explained through the formation of additional hydrogen bonds that prevent optimal fitting of substrate in the active site. This is visible from the differences in O–N1 interactions at the larger distances (from 15.2 to 17.2 Å), where 5'-

-AMPN forms hydrogen bonds while AMP cannot establish these interactions with the environment.

Table with structures and K_d values used in the study is presented in Table S-I, as well as in figures connected with the preliminary QSAR studies: TIP–TIP interactions for ADP and APS, and TIP-TIP probe heatmap for ADP, AMP and APS (Fig. S-1 of the Supplementary material), the location of favorable hydrophobic interactions of ADP mapped using DRY probe (Fig. S-2 of the Supplementary material), differences in DRY-DRY interactions that ADPβF and ADPβS form with target and differences in TIP-TIP interactions ADPαS and ADP (Fig. S-3 of the Supplementary material), DRY–DRY interactions that ADPβS and ADPβF form with enzyme (Fig. S-4 of the Supplementary material), differences in DRY-DRY interactions between APS and APSαS, and APS and APSβM (Fig. S-5 of the Supplementary material), TIP–TIP interactions for AMPCF2P and AMPNP (Fig. S-6 of the Supplementary material), TIP-TIP interaction 5'-AMPS and AMP and O–N1 interaction 5'-AMPN and AMP (Fig. S-7 of the Supplementary material) and the structural features associated with the additional variables positively and negatively correlated with the APS reductase inhibitory activity (Fig. S-8 of the Supplementary material).

Partial least square regression model

To establish the quantitative relation between the biological activity and computed GRIND descriptors, partial least square (PLS) regression was applied. The optimum model, by means of r^2 and q^2, was generated using 3 latent variables (LV). Further increase in the number of LV didn't improve the statistical quality of the model. Statistically acceptable models are those with $r^2 > 0.5$ and $q^2 > 0.9$.

The statistical parameters of the developed model are shown in Table I.

TABLE I. The statistics of PLS model developed for the APS reductase inhibitory activity of APS analogues; *SSX* – *X* variable explanation; *SSXacc* – *X* accumulation (cumulative value); *SDEC* – standard deviation of error of calculation; *SDEP* – standard deviation of error of prediction; r^2acc – r^2 accumulation; q^2acc – q^2 accumulation

LV	*SSX*	*SSXacc*	*SDEC*	*SDEP*	$r^{2\#a}$	r^2acc$^{\#b}$	q^2acc$^{\#c}$
1	30.75	30.75	0.89	1.15	0.52	0.52	0.19
2	21.05	51.8	0.57	0.95	0.28	0.8	0.44
3	7.7	59.51	0.37	0.94	0.12	0.92	0.46
4	9.92	69.42	0.27	0.94	0.04	0.96	0.46
5	4.23	73.66	0.18	0.98	0.03	0.98	0.41

From the PLS scores plot (Fig. 2) several variables positively and negatively correlated with the biological activity are observed.

The most significant variables obtained in PLS analysis are presented in Table II. Each variable represents the product of interaction energies of two

chemical probes at certain distance. PLS correlates these variables with biological activity where positive variable values indicate positive influence on biological activity and vice versa.

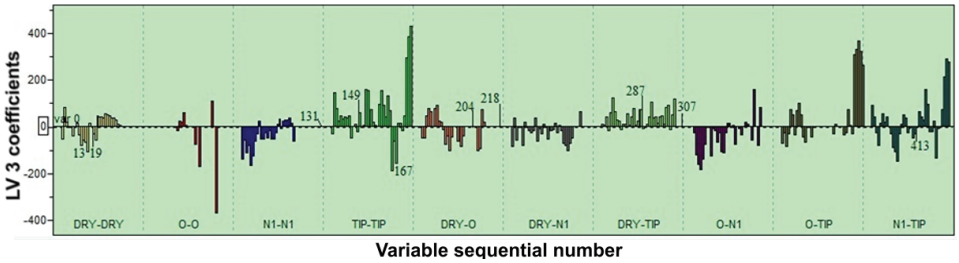

Fig. 2. PLS scores plot for 3LV model where the most significant variables are labeled.

TABLE II. The most significant variables obtained by PLS analysis

Variable	Distance, Å	Correlogram	The influence on activity
13	5.2-5.6	DRY–DRY	Negative
19	7.6-8.0	DRY–DRY	Negative
149	3.2-3.6	TIP–TIP	Positive
167	10.4-10.8	TIP–TIP	Negtive
287	2.0-2.4	DRY–TIP	Positive
393	16.4-16.8	O–TIP	Positive
413	14.8-15.2	N1–TIP	Negative

CONCLUSION

Concerning that APSR is essential for the survival of mycobacteria in latent phase of infection, discovery of small molecules that would inhibit its action is of interest for the development of new potential antituberculotics. In this study, the set of synthetized ligands for APSR was studied using 3D QSAR methodology with the descriptors derived from MIFs. Compounds from the data set, 16 analogues of natural substrate, were classified on the base of structural similarity, into three main groups: 1) AMP and analogues, 2) ADP and analogues and 3) APS and analogues.

Significant differences in APSR inhibitory activity, probed on DRY, O, N1 and TIP interactions, were observed between three classes of compounds, indicating that slight differences in structure leads to significant changes in protein–ligand binding. Studies showed the differences of analogues in shape complementarity. Interactions with active site were also influenced by modifications in α and β positions, charge, size and polarizability of groups and atoms, conformational freedom, as well as protonation at physiological pH. Quantitative relation between biological activity and computed GRIND descriptors was established by partial least square (PLS) regression. The optimum model (r^2acc = 0.92 and

q^2acc = 0.46) was generated using 3 latent variables (LV). The most significant variables obtained in PLS analysis were further interpreted.

SUPPLEMENTARY MATERIAL

Additional data are available electronically at the pages of journal website: https://www.shd-pub.org.rs/index.php/JSCS/index, or from the corresponding author on request.

Acknowledgement. This work was supported by Ministry of Science, Education and Technological Development of Republic of Serbia under contract with University of Belgrade – Faculty of Pharmacy (No 451-03-9/2021-14/200161) and Innovation Center of the Faculty of Chemistry, University of Belgrade (No 451-03-68/2020-14/200168).

ИЗВОД

3D-QSAR СТУДИЈА АНАЛОГА АДЕНОЗИН 5'-ФОСФОСУЛФАТА (APS) КАО ЛИГАНДА ЗА APS РЕДУКТАЗУ

СЛАВИЦА ЕРИЋ[1], ИЛИЈА ЦВИЈЕТИЋ[2] и МИРЕ ЗЛОХ[3,4]

[1]Универзитет у Београду, Фармацеутски факултет, Војводе Степе 450, 11 221 Београд, Србија; [2]Универзитет у Београду, Иновациони центар Хемијског факултета, Студентски трг 12-16, 11 000 Београд, Србија; [3]Nanopuzzle Medicines Design, Stevenage, United Kingdom; [4]Фармацеутски факултет, Универзитет Привредна Академија, Нови Сад, Србија

Метаболизам сумпора (пут асимилације сумпора, SAP) један је од кључних путева за патогенезу и преживљавање *Mycobacterium tuberculosis* (Mtb) у латентном периоду. Аденозин 5'-фосфосфат редуктаза (APSR) је значајан ензим који је укључен у SAP, не налази се у људском организму и може бити валидно циљно место за развој нових антитуберкулотика. Циљ овог рада је развој 3D-QSAR модела који се заснива на кристалној структури APSR из *Pseudomonas aeruginosa*, који има висок степен хомологије са APSR из Mtb, у комплексу са супстратом, аденозин 5'-фосфосулфатом (APS). 3D-QSAR модел је постављен коришћењем сета 16 нуклеотидних аналога APS применом дескриптора независних од полазних тачака, изведених из поља молекуларних интеракција (MIF). Модел служи за боље разумевање кључних карактеристика молекула неопходних за интеракцију са циљним местом, у сврху рационалног дизајнирања малих молекула, инхибитора APSR из Mtb.

(Примљено 28. новембра 2020, ревидирано 21. јануара, прихваћено 26. фебруара 2021)

REFERENCES

1. R. Schnell, G. Schneider, *Biochem. Biophys. Res. Comm.* **396** (2010) 33 (https://doi.org/10.1016/j.bbrc.2010.02.118)
2. O. Poyraz, K. Brunner, B. Lohkamp, H. Axelsson, L. G. J. Hammarström, R. Schnell, G. Schneider, *PLOS ONE* **10** (2015) e0121494 (https://doi.org/10.1371/journal.pone.0127016)
3. R. Iwanicka-Nowicka, A. Zielak, A. M. Cook, M. S. Thomas, M. M. Hryniewicz, *J. Bacteriol.* **189** (2007) 1675 (https://doi.org/10.1128/JB.00592-06)
4. P. B. Palde, A. Bhaskar, L. E. Pedro Rosa, F. Madoux, P. Chase, V. Gupta, T. Spicer, L. Scampavia, A. Singh, K. S. Carroll, *ACS Chem. Biol.* **11** (2015) 172 (https://doi.org/10.1021/acschembio.5b00517)
5. J. A. Hong, D. P. Bhave, K. S. Carroll, *J. Med. Chem.* **52** (2009) 5485 (https://doi.org/10.1021/jm900728u)

6. S. K. Hatzios, C. R. Bertozzi, *PLOS Pathog* **7** (2011) e1002036 (https://doi.org/10.1371/journal.ppat.1002036)
7. S. Cosconati, J. A. Hong, E. Novellino, K. S. Carroll, D. S. Goodsell, A. J. Olson, *J. Med. Chem.* **51** (2008) 6627 (https://doi.org/10.1016/j.biotechadv.2011.08.021)
8. H. Wieman, K. Tøndel, E. Anderssen, F. Drabløs, *Mini Rev. Med. Chem.* **4** (2004) 79 (https://doi.org/10.2174/1389557043403639)
9. *OMEGA 2.5.1.4: OpenEye Scientific Software*, Santa Fe, NM (http://www.eyesopen.com)
10. P. C. D. Hawkins, A. G. Skillman, G. L. Warren, B. A. Ellingson, M. T. Stahl, *J. Chem. Inf. Model.* **50** (2010) 572 (https://doi.org/10.1021/ci100031x)
11. ROCS 3.2.1.4: OpenEye Scientific Software, Santa Fe, NM (http://www.eyesopen.com)
12. P. C. D. Hawkins, A. G. Skillman, A. Nicholls, *J. Med. Chem.* **50** (2007) 74 (https://doi.org/10.1021/jm0603365)
13. M. Pastor, G. Cruciani, I. McLay, S. Pickett, S. Clementi, *J. Med. Chem.* **43** (2000) 3233 (https://doi.org/10.1021/jm000941m)
14. J. Chartron, K. S. Carroll , C. Shiau, H. Gao, J. A. Leary, C. R. Bertozzi, C. David Stout C. *J. Mol. Biol.* **364** (2006) 152 (https://doi.org/10.1016/j.biotechadv.2011.08.021).